Hydrology and Earth System Sciences Discussions

Sediment transport modelling in a distributed physically based hydrological catchment model

M. Konz[1], **M. Chiari**[2], **S. Rimkus**[1], **J. M. Turowski**[3], **P. Molnar**[1], **D. Rickenmann**[3], and **P. Burlando**[1]

[1]Institute of Environmental Engineering, Hydrology and Water Resources Management, ETH Zurich, Wolfgang-Pauli-Straße 15, 8093 Zurich, Switzerland
[2]Institute of Mountain Risk Engineering, University of Natural Resources and Life Sciences, Peter Jordanstraße 82, 1190 Vienna, Austria
[3]Mountain Hydrology and Torrents, Swiss Federal Research Institute, WSL, Zürcherstraße 111, 8903 Birmensdorf, Switzerland

Correspondence to: M. Konz (markus.konz@ifu.baug.ethz.ch)

Abstract

Sediment transport and erosion processes in channels are important components of water induced natural hazards in alpine environments. A distributed hydrological model, TOPKAPI, has been developed to support continuous simulations of river bed erosion and deposition processes. The hydrological model simulates all relevant components of the water cycle and non-linear reservoir methods are applied for water fluxes in the soil, on the surface and in the channel. The sediment transport simulations are performed on a sub-grid level, which allows for a better discretization of the channel geometry, whereas water fluxes are calculated on the grid level in order to be CPU efficient. Flow resistance due to macro roughness is considered in the simulation of sediment transport processes. Several transport equations as well as the effects of armour layers on the transport threshold discharge are considered. The advantage of this approach is the integrated simulation of the entire water balance combined with hillslope-channel coupled erosion and transport simulation. The comparison with the modelling tool SETRAC and with LiDAR based reconstructed sediment transport rates demonstrates the reliability of the modelling concept. The modelling method is very fast and of comparable accuracy to the more specialised sediment transport model SETRAC.

1 Introduction

Bedload transport in rivers is a problem of considerable scientific and public concern. During the course of heavy rain events significant masses of sediment can be mobilized and transported downstream. The consequences include reservoir siltation, blocking of channels which can cause flooding, loss of aquatic habitat and river bank instabilities. Especially in mountainous catchments with channel gradients larger than 0.05 and bed sediment containing a high portion of gravel, cobbles and boulders, transport capacities during flood events can reach very high values and the limiting factor is often

only the sediment availability. The channel geometry varies largely as well as stream flow velocity and roughness (Hassan et al., 2005). Thus, sediment transport dynamics in these channels may substantially differ from those in low-gradient channels. Due to the socio-economic relevance of sediment transport processes for their potential of wa-

5 ter induced natural hazards, accurate simulation and forecasting tools are required. A considerable number of bedload transport models have been developed in the recent decades but most of them have not been tested for steep channels in torrents. Two strategies can be followed for sediment routing in steep channels. The first approach consists in using a hydraulic simulation model including a sediment transport module,

10 which allows variations in bed geometry due to erosion or deposition processes to be considered. These models typically include the full Saint Venant equations for one- or two-dimensional flow combined with a sediment transport equation together with the so-called Exner equation to account for sediment transport and storage effects in the riverbed. Examples are the one dimensional 3ST1D model (Papanicolaou et al.,

15 2004), the 1.5 dimensional FLORIS-2000 model (Reichel et al., 2000) or the semi two-dimensional stream tube SDAR model (Bahadori et al., 2006). Most two-dimensional bedload transport models have been developed for large riverine or estuarine envi-ronments. An example of a two-dimensional model applicable for steep slopes is the Flumen model (Beffa, 2005). The SETRAC model (Rickenmann et al., 2006; Chiari

20 et al., 2010) has specifically been developed for simulations of steep alpine torrents. These very specialized models allow for simulations of sediment transport in a detailed way. The drawback of these models is that important feedback mechanisms as well as the seriality of processes are hard to study due to the separate treatment of the water cycle and the sediment transport. The answer to this limitation can come from

25 integrated models, which account for both basin hydrology and processes driven by hy-drological response like soil slips and sediment transport in channels. Thus, a second group of hydro-sedimentologic models considers sediment transfer processes at the catchment scale, within the framework of a hydrological water cycle model. Examples are the ETC rainfall-runoff-erosion model (Mathys et al., 2003), the SHESED model

Distributed physically based hydrological catchment model

M. Konz et al.

Title Page

Abstract	Introduction
Conclusions	References
Tables	Figures

◀◀	▶▶
◀	▶
Back	Close

Full Screen / Esc

Printer-friendly Version

Interactive Discussion

Distributed physically based hydrological catchment model

M. Konz et al.

(Wicks and Bathurst, 1996), the DHSVM model (Doten et al., 2006) or the Promab-GIS model (Rinderer et al., 2009).

Models for simulations of mountainous catchments require specific modules for simulation of hydrological processes such as snow and glacier melt and routing, while a detailed description of the highly variable channel geometry is needed for the sediment transport simulations. In fact, geometrical properties like channel bed slope and channel width are important parameters which control the hydraulics and consequently the bedload transport. Usually, a high resolution grid is a prerequisite for the detailed description of channel geometry. However, model simulations demand more CPU with increasing resolution and basin wide simulations become inefficient and slow. In this paper we added to the distributed physically-based hydrological model TOPKAPI a module for the simulation of the temporal evolution of river bed sediment dynamics at the catchment scale. The innovative aspect of the newly introduced sediment module is the sub-grid simulation of the sediment routing, which takes advantage of the more detailed description of the channel geometry at the sub-grid level, and the efficient hydrological and hydraulic simulations on the coarser grid level. This paper describes the implementation of the sub-grid sediment modelling scheme and demonstrates its ability to simulate well documented flood events in the Bernese Alps, Switzerland.

2 Study site and extreme event in August 2005

Many regions in Austria, Switzerland and Germany were affected by the flood events in August 2005 (MeteoSchweiz, 2006). A massive cyclone over the northern part of Italy caused heavy rainfall particularly from 21–22 of August 2005. The period of relevant precipitation was about four days, whereas thunderstorms were not of major importance. In Switzerland the whole north-alpine region was affected by heavy rainfall that triggered widespread flooding. The highest precipitation sums for a 72 h period were measured in Switzerland (more then 250 mm: in Gadmen: 320 mm, Rotschalp: 283 mm, Weesen: 277 mm and Amden: 267 mm) (MeteoSchweiz, 2006).

For testing of the newly developed sediment transport routine in TOPKAPI we selected the Chiene catchment in the Bernese Alps that was heavily affected by the storm event. The catchment is situated in the Canton Berne, the catchment area is 90.5 km^2 and is drained by the main river Chiene and the tributary Spigge (see Fig. 1).

No streamflow measurements for the Chiene mountain river are available, but the discharge has been reconstructed with streamflow measurements upstream and downstream of the confluence with the river Kander (LLE Reichenbach, 2006; Fig. 1). There is one gauging station 6 km downstream (Hondrich) and one 6 km upstream (Frutigen) at the river Kander.

The Chiene is a steep mountain stream with a mean channel gradient of 0.05. The slope is ranging from 0.004 in the flat middle reaches up to 0.17 in the steepest reaches (Fig. 2c). The channel width has a maximum of around 150 m between 5.5 and 6.2 km. The initial sediment storage depth was estimated in the field at 1 to 5 m. The grain size distributions were estimated with a transect-by-number analysis and evaluated after Fehr (1987), values were taken from Chiari et al. (2010).Two LiDAR based digital elevation models are available for the catchment, representing the pre- and post- flood situation. Morphologic changes in torrents and mountain rivers are only caused by major flood events. No other flood events have been reported for the time span between the two LiDAR flights. Topographic change is due to the divergence in sediment transport flux and can be calculated using the Exner equation (Eq. 1):

$$\left(1 - \lambda_p\right) \frac{d\eta}{dt} = -\frac{dq_s(x)}{dx} + p_b(x) \tag{1}$$

where η is the bed elevation, λ_p is the porosity, $q_s(x)$ is the downstream sediment flux, and $p_b(x)$ accounts for lateral sediment inputs. To calculate bedload flux at some location $x = L$, Eq. (1) can be integrated as

$$q_s(L) = q_s(0) + \int_0^L \left(p_b(x) - \left(1 - \lambda_p\right)\frac{d\eta}{dt}\right) dx \tag{2}$$

Equation (2) shows that the sediment flux at L is the sum of the sediment flux at the most upstream location ($x = 0$), the integrated lateral sediment inputs everywhere upstream of L, and the integrated elevation change along the bed. From differencing the topographic profiles, we have calculated the last term of Eq. (2) (the integrated elevation change). The volumes were corrected for the pore volumes and the amount of fine sediment transported as suspended load further downstream. For this study it is assumed that the pore volume and the content of the sediment makes up about 50% of the erosion volumes. For depositional situations 30% pore volume is considered. It is assumed that suspended sediment and washload are transported farther downstream.

The volumetric analysis was compared qualitatively with aerial photographs and completed with data from sediment redistribution during the flood recovery phase (LLE Reichenbach, 2006). During the event, about $120\,000\,\text{m}^3$ of bedload were mobilized. Most of the material was deposited in the flat middle reaches (km 5.3 to km 6) and in the village of Kien (close to the confluence with Kander river). The LiDAR analysis indicated that there was more deposition in the flat middle reaches (km 5.5) than sediment input from upstream areas not covered by the LiDAR flight. Therefore, a sediment input from that area of about $20\,000\,\text{m}^3$ (at km 8.3 in Fig. 2a) was considered, which is in agreement with field observations (LLE Reichenbach, 2006). The advantage of this method is the coverage of the whole area.

3   The TOPKAPI model

TOPKAPI has originally been developed at the University of Bologna (Italy) as a physically based distributed hydrological catchment model (Todini and Ciarapica, 2001; Liu and Todini, 2002; Liu et al., 2005). The model simulates all relevant components of the water balance and transfers the rainfall-runoff processes into non-linear reservoir equations, which represent drainage of the soils, overland flow and channel flow. The relevant information about topology, surface roughness and soil characteristics are obtainable from soil maps, digital elevation models and land use maps.

Distributed physically based hydrological catchment model

M. Konz et al.

The Hydrology and Water Resources Management group of ETH Zurich, Switzerland, has further developed TOPKAPI to make it applicable to high alpine regions. A new snow and ice melt routine has been implemented that enables the distributed simulation of snow accumulation and melt as well as glacier melt. Apart from the modifications of the water cycle simulations, modules to simulate water induced geomorphological processes like soil slips, hillslope erosion and channel sediment transport have been implemented in the model. In the following a brief overview of the model's water cycle components will be given and the channel sediment transport module will be described in detail.

3.1 The water cycle components in TOPKAPI

The water cycle components can by grouped into four major routines: (i) the regionalization routine for meteorological input variables, (ii) the snow and glacier routine, (iii) the soil routine, and (iv) the channel routine. The water cycle is simulated in a distributed grid-based approach and within one time step the model simulates water cycle components for each grid cell in the downstream direction. Meteorological input variables (temperature and precipitation) can be provided as maps or as point measurements. Vertical lapse rates are used in the regionalization routine to generate spatial temperature and precipitation fields if point measurements are provided.

TOPKAPI computes potential clear-sky global irradiance for melt simulation based on the procedure described by Corripio (2003). Cloudy conditions are accounted for by a parameterisation of the cloud factor as described in Pellicciotti et al. (2005) which is based on an empirical relationship using the temperature range over a day. The melting of snow and ice is computed if the air temperature T_i (°C) exceeds the threshold air temperature TT using the enhanced temperature-index model of Pellicciotti et al. (2005), which represents the energy balance in a conceptual way (Eq.!3).

$$M_i = TF \times T_i + SRF \times I_{G\downarrow_i} \times (1 - al_i), \tag{3}$$

where M_i is melt in mm water equivalent (w.e.) h^{-1} of cell I, TF is the Temperature Factor in mm w.e. K^{-1} h^{-1}, SRF is the Shortwave Radiation Factor in mm w.e. m^2 W^{-1} h^{-1}. I_{G_i} is global irradiance in Wm^{-2}, and al_i is the surface albedo.

The albedo in the model can be different for ice and snow and the snow albedo evolves with the age of the snow pack (Brock et al., 2000). The ice albedo is defined to be space and time invariant. All runoff emerging from glaciated grid cells is added either to a snow melt reservoir, in the case of snow melt and rain on a snow covered cell, or to an ice melt reservoir, in the case of ice melt or rain on a snow free but glaciated cell. Thus, each glacier or glacier group is represented by two linear reservoirs, one for snow and one for ice melt plus rain input. The outflow of both reservoirs is then controlled by a linear reservoir approach as described for example by Ven Te Chow et al. (1988) and Hock and Noetzli (1997). Outflow of the glacier reservoir is directed to the surface and routed from there as on not glaciated cells. Water from snow melt and rain infiltrates into the soil unless the soil is already saturated. Together with inflowing water from upstream and lateral cells, this vertical infiltration constitutes the soil water content.

Overland flow occurs if the maximum soil water storage is exceeded. This is equivalent to the saturation excess processes of runoff generation. Actual evapotranspiration is calculated as a function of the soil water content and potential evapotranspiration if the water content is below a certain threshold. Otherwise, actual evapotranspiration equals the potential evapotranspiration, which is computed based on the Makkink approach (Deyhle et al., 1996).

Water fluxes in the soil are obtained by combining the dynamic equation (Eq. 4) with the equation for continuity of mass (Eq. 5).

$$q = \tan(\beta)\, k_s\, L\, \Theta^b \tag{4}$$

$$p = (\vartheta_s - \vartheta_r)\, L\, \frac{\partial \Theta}{\partial t} + \frac{\partial q}{\partial x} \tag{5}$$

Title Page

Abstract | Introduction

Conclusions | References

Tables | Figures

|◄ | ►|

◄ | ►

Back | Close

Full Screen / Esc

Printer-friendly Version

Interactive Discussion

Here q is the horizontal flow in the soil in $m^2\,s^{-1}$, p is the intensity of vertical inflow in $m\,s^{-1}$, t is time in s, x is the direction of flow along a cell in m, β is the slope angle as radiance, b is an empirical parameter which depends on the soil characteristics, k_s is the saturated hydraulic conductivity in $m\,s^{-1}$, L is the thickness of the soil layer in m, Θ is the mean value along the vertical profile of the soil water content, ϑ_s is the saturated soil water content and ϑ_r is the residual soil water content.

Two soil layers can be used to simulate interflow and base flow components. Surface runoff is computed with a comparable approach but Manning's formula is used as a dynamic equation. Water routing in the channel is particularly important for sediment transport simulations and is therefore described in detail in the next section.

The simulated soil components are further utilized to compute the factor of safety, which is an indicator for slope failure due to increased pore pressure. Soil erosion on hillslopes is computed based on simulated overland flow. The focus of this paper is set on sediment transport simulations during flood events. The hillslope erosion module is not discussed here.

3.2 Channel water routing

Channel flow is described with a kinematic wave approximation similar to overland flow using Manning's formula (Eq. 6) and the continuity equation shown in Eq. (7). The channels are assumed to be rectangular.

$$q_c = \frac{1}{n_c}\sqrt{S}\left(\frac{B^{2/3}}{C}\,By_c^{5/3}\right) \tag{6}$$

$$\frac{\partial V_c}{\partial t} = \left(r_c + Q_c^u\right) - q_c \tag{7}$$

where q_c is the horizontal flow in the channel in $m^3\,s^{-1}$, n_c Manning's friction coefficient for channel roughness in $m^{-1/3}\,s$, S is the bed slope, B is the channel width in m, C is

Distributed physically based hydrological catchment model

M. Konz et al.

the wetted perimeter, y_c is the water depth in the channel in m, V_c is the water volume in the channel in m^3, t is time in s, r_c is the lateral drainage input in m^3 s^{-1}, Q_c^u is the inflow discharge from the channel reach of the upper cells in m^3 s^{-1}.

The three non-linear reservoir equations representing soil flow, overland flow and channel flow can be solved analytically as discussed in detail by Todini and Mazzetti (2008). This enables a very efficient computation of the flow processes.

Flow resistance due to grain roughness plays a crucial role in steep headwater streams and is considered in TOPKAPI by a variable Manning friction coefficient. The Manning coefficient depends on the flow depth and is therefore expressed as a function of discharge, bed slope and the characteristic grain size of the channel bed material (Rickenmann, 1994, 1996). The equations to estimate the roughness coefficient in TOPKAPI are:

$$n_c = \frac{S^{0.19} \, d_{90}^{0.64}}{0.97 \, g^{0.41} \, q_c^{0.19}} \text{ for } S \geq 0.008 \tag{8}$$

and

$$n_c = \frac{S^{0.03} \, d_{90}^{0.23}}{4.36 \, g^{0.49} \, q_c^{0.02}} \text{ for } S \leq 0.008 \tag{9}$$

where g is the gravity acceleration in ms^{-2} and d_{90} is the grain size of the bed material for which 90% of the bed material is finer by weight.

Discharge is simulated per grid cell that is assigned as a channel cell. In TOPKAPI the cell length is automatically the length of the river section in this cell, whereas the channel width can be defined as a fraction of the cell size. The slope of the bed is derived from the DEM.

3.3 Sediment transport in TOPKAPI

3.3.1 The sub-grid modelling scheme

TOPKAPI uses square raster cells for spatial discretization and the rivers are represented as predefined sections of the raster cells with a constant width (Fig. 3a). For
sediment transport simulations this discretization of the channel is generally too coarse. Therefore, sub-grid cross-sections of different length and width can be used within each grid cell and different properties can be assigned to these cross-sections (Fig. 3b). The properties are width, length, initial sediment storage depth, slope and grain size distribution. Discharge is simulated on the grid cell level (Fig. 3a) and is assumed to
be constant for all sub-grid cross-sections (stationary conditions within a time step, Fig. 3b). There is no feedback mechanism between sediment transport simulations and hydraulic simulations, which means that for the hydraulic simulations the channel geometry is constant through time.

In order to avoid rapid exhaustion of the sediment storages the time step length can
be decreased as a fraction of the global time step used for the hydrological simulations.

3.3.2 Sediment transport capacity

For the calculation of the sediment transport capacity various bedload transport formulas and adjustment methods can be selected in order to adapt the model to the catchment conditions. In the following we provide the equations of the setups used to
simulate a storm event in August 2005 in the Chiene catchment, Bernese Alps (see Sect. 1 for the description of the event).

Only a limited number of bedload formulas have been developed for steep gravel streams mainly in laboratory flumes. The following formula (Rickenmann, 1991, 2001) is selected to estimate the transport capacity (q_{pot} in m^2 sediment s^{-1}):

$$q_{pot} = 3.1 \left(\frac{d_{90}}{d_{30}}\right)^{0.2} \left(q_{c,s}(t) - q_{crit}\right) S^{1.5} (s-1)^{-1.5} \tag{10}$$

where d_{30} is the characteristic grain size for which 30% by weight is finer, $q_{c,s}(t)$ is the specific discharge in $m^2 s^{-1}$, q_{crit} is the specific critical discharge $m^2 s^{-1}$ and s the ratio between sediment and fluid density ($s = \rho_s/\rho_f$).

Sediment transport starts once the critical discharge is exceeded. A number of formulations exist to estimate the critical discharge. In TOPKAPI five different formulae are available and the following formulae according Rickenmann (1990), were chosen for the simulations:

$$q_{crit} = 0.065 (s - 1)^{1.67} g^{0.5} d_{50}^{1.5} S^{-1.12} \tag{11}$$

$$q_{crit} = 0.143 (s - 1)^{1.67} g^{0.5} d_{65}^{1.5} S^{-1.167} \tag{12}$$

For steep mountain streams with irregular bed topography and low relative flow depth additional flow resistance due to macro-roughness elements at the bed becomes important. However, the above described sediment transport formulae are generally based on flume experiments with rather uniform bed material where the moveable bed had a more or less planar surface without bed form structures. Thus, essentially skin drag was present in these experiments. In steep and rough streams the total flow resistance is considerably increased. This could be a reason why the bedload transport formulae often overestimate observed bedload transport, if they are applied to steep and rough channels. Energy losses due to form roughness can therefore be considered optionally in the model by introducing a reduced energy slope (Chiari, 2008; Chiari et al., 2010).

$$\frac{n_o}{n_c} = \frac{0.0756 \, q_c^{0.11}}{g^{0.06} \, d_{90}^{0.28} \, S^{0.33}} \tag{13}$$

$$\frac{n_o}{n_{tot}} = 0.092 \, S^{-0.35} \left(\frac{y_c}{d_{90}}\right)^{0.33} \tag{14}$$

$$S_{red} = S \left(\frac{n_o}{n_c}\right)^{\alpha} \tag{15}$$

Distributed physically based hydrological catchment model

M. Konz et al.

Title Page

Abstract	Introduction
Conclusions	References
Tables	Figures

⏮ | ▶️

◀ | ▶

Back | Close

Full Screen / Esc

with a roughness coefficient n_o associated with a base-level flow resistance only, and n_c corresponds to the total flow resistance.

According to the Manning-Strickler equation an appropriate value of the exponent a in Equation 15 should be $a = 2$. Meyer-Peter and Mueller (1948) showed theoretically that the exponent α may vary between 1.33 and 2.0, and from their experiments they empirically determined a value of 1.5. To adapt the reduction of the energy slope to observations of bedload transport, the exponent in Eq. (15) can be varied between the values 1 and 2 (Rickenmann et al., 2006). Therefore a can be used as a calibration parameter within the specified range. Back-estimation of a from bedload data for the Austrian and Swiss flood events in 2005 resulted in a best fit exponent a in the range of about 1.2 to 1.5 (Chiari, 2008). Mountain streams can develop an armour layer if finer sediment fractions are more likely to be transported than coarser fractions. If armouring cannot be neglected this effect can be considered optionally (alternatively to form drag) in combination with the modified critical discharge $q_{\text{crit,a}}$ (Badoux and Rickenmann, 2008). As shown in Eq. (16) the specific critical discharge, q_{crit}, is increased and thus the incipient motion is delayed, which causes reduced sediment transport rates.

$$q_{\text{crit,a}} \;=\; q_{\text{crit}} \left(\frac{d_{90}}{d_m} \right)^{10/9} \tag{16}$$

with d_m as the mean grain size.

The sediment transport capacity finally is the maximum amount of sediment that can be transported by the water discharge considering losses due to form roughness or effects of armouring layers.

The actual sediment transport is subject to sediment availability in the sediment storage. The sediment budget per sub-grid cross-section is calculated based on the discrete balancing of incoming sediment, sediment transport capacity and available sediment in the storage (Eq. 17).

$$\frac{\partial h}{\partial t} \;=\; -\frac{\partial q_s}{\partial l} \tag{17}$$

where q_s is the specific transported sediment volume in $m^2 s^{-1}$, h is the sediment depth in m and l is the length of the current cross-section in m.

Therefore, erosion and deposition can be simulated accordingly. If the calculated transport capacity exceeds the sediment input from the upstream section, erosion oc-
5 curs as long as sediment is available in the storage. Erosion is limited by the predefined depth of the sediment layer.

The actually transported sediment is directed to the next downstream cross-section. If the sediment input into the section is larger than the transport capacity, deposition occurs and the sediment storage is filled. During deposition it is possible that the river
10 section becomes blocked and the discharge cannot flow through the section any more. This can especially occur at points with significant changes of the channel slope. If this problem occurs the additional volume that blocks the section is added to the next downstream cell (Fig. 4) and the slope is set to a predefined value of 0.1%.

After each time step the slope of each cross-section is recalculated according to the
15 following formula in order to simulate a mobile river bed:

$$S = \frac{h_{up} - h_{dn}}{l_{dn}/2 + l_{up}/2 + l} \qquad (18)$$

where $h_{dn,up}$ are the downstream and upstream river bed heights in m and $l_{dn,up}$ are the downstream and upstream cross-section lengths in m.

The newly defined slope is then used for transport simulations in the next time step.

20 **4   The SETRAC model**

In Sects. 4 and 5 TOPKAPI is compared to the more sophisticated specialised sediment transport model, Sediment TRAnsport in Alpine Catchments (SETRAC). SETRAC is briefly described here, especially the differences between TOPKAPI and SETRAC are discussed. SETRAC is a one-dimensional model for the simulation of sediment trans-
25 port in torrents and mountain rivers and was developed at the University of Natural

Resources and Applied Life Sciences, Vienna (BOKU), Austria (Rickenmann et al., 2006; Chiari et al., 2010). The model has been thoroughly tested against laboratory flume data and well documented field events by Chiari (2008), Chiari et al. (2010). The channel network is represented by nodes, cross-sections and sections. Nodes con-
5 tain the information about the location of the related cross-sections. Cross-sections are described by pairs of points containing information about the distance from the left bank and the altitude. Each slice of the cross-section can be of the type main channel, bank or riparian. This discretization allows a detailed description of the cross-section geometry.
10 Erosion and deposition, as well as bedload transport can only occur in slices of the type main channel. Each cross-section contains information about the grain size distribution, the sediment storage depth and the initial slope. Input hydrographs can be assigned to cross-sections as time series. Sediment input as time series is also possible. For calculations, the cross-sections are connected by strips to get a representative
15 discretization of the channel. The number of strips depends on the number of slices that are used to specify a cross-section, implying that the number of strips increases with the complexity of the cross-section. Discharge and bedload transport is calculated separately for each strip of the cross-section. The input hydrographs are routed using the kinematic wave approach that is solved numerically by an explicit finite difference
20 method with an upwind scheme. The same sediment transport simulation methods as discussed in the previous section can be used in SETRAC, however SETRAC additionally allows for a fractional bedload transport. Feedback mechanisms of the changing river bed geometry on hydraulic simulations are possible, which is not the case in TOP-KAPI. The interested reader is referred to Chiari (2008) and Chiari et al. (2010) for more
25 detailed descriptions of SETRAC.

5 Simulation of the 2005 event with TOPKAPI and SETRAC

For the simulations, the Chiene as well as the most important tributary Spigge were considered. In total, 9.77 channel km were simulated (8.24 km Chiene and 1.44 km Spigge). TOPKAPI was forced with point information of the meteorological input data temperature and precipitation taken from a meteorological station in Adelboden around 16 km in the South-West of the catchment, which were redistributed with the help of lapse rates. Total event duration of 60 h was simulated for different model setups as described in Table 1 using the geometrical information of Fig. 2c, the initial storage depths of Fig. 2b and the grain size distribution provided by Chiari et al. (2010). 3600 sub-time steps were taken for the temporal discretization of the sediment routing, which corresponds to a time step length of 1 s compared to 1 h for the hydrological simulations. The sub-grid cross-sections in TOPKAPI were assigned to the grid cells according to the location of the cross-sections resulting in a non-uniform distribution of sub-grid sections in the grid cells. However, an equal spacing between the sub-grids of 50 m was assumed even if only one sub-grid is assigned to a grid cell. The grid cell size is 250×250 m^2.

The major goal of this study is to compare the two models. Therefore, the hydrologic calibration of TOPKAPI was done in a way that both models deliver comparable discharge simulations and the reconstructed discharge of the 2005 event was only used to demonstrate the right order of magnitude of the simulations (Fig. 5). The model parameters of the snow and glacier routine and the soil routine have been calibrated solely against discharge values because this is the most important component of the water cycle to simulate sediment transport in the channel. Simulations were done for the entire year 2005 and initial conditions for the sediment simulations of the 60 h event were taken from these simulations.

The same cross-sections as in SETRAC were used for TOPKAPI and assigned to the corresponding raster cells. At the confluence point of Spigge and Chiene, one raster cell covers cross-sections of both rivers. The real confluence point is further

downstream but due to the spatial resolution of the grid the confluence point is simulated further upstream. Thus, the simulated discharge of this raster cell represents already the merged rivers and therefore is much higher than the discharge of the Spigge cross-sections. In order to avoid overestimations of sediment transport capacities, the cross-sections of Spigge were shifted upstream by one cell and the sediment output of the last Spigge cross-section is added to the correct cross-section of the Chiene. This modification allows for a more realistic simulation of the hydraulic conditions in the sub-grid cross-section.

Simulated discharge values of the grid cells were used for each cross-section within the grid cell. However, the hydraulics were simulated using the original slopes of the grid cell and no feedback mechanisms of the mobile bed on the discharge simulations were considered in TOPKAPI.

Radar precipitation data were used in order to generate the input hydrographs needed for the SETRAC simulations. The hydrologic model HEC-HMS has been calibrated to match at least the magnitude of the reconstructed hydrograph (LLE Reichenbach, 2006). Discharge simulations compare well between TOPKAPI and SETRAC, which is a prerequisite for the comparison of the sediment transport simulations (Fig. 5). For the spatial discretisation every 50 m a cross-section was derived from the digital elevation model, which was generated by airborne LiDAR before the extreme event occurred. The HEC-HMS hydrographs were assigned to the nodes of SETRAC according to predefined sub-catchments.

Figure 6 shows a comparison of SETRAC and TOPKAPI simulations with the accumulated bedload transport recalculated from the morphological changes. The time integrated bedload transport volumes are shown for the main channel (Chiene). The simulations of TOPKAPI and SETRAC with full transport capacity (M1, Table 1) deliver comparable results but overestimate the reconstructed bedload transport. TOPKAPI produces slightly lower bedload transport than SETRAC especially in the downstream part of the Chiene between 0.8 and 2 km. The contribution of the Spigge can be noticed at 6 km in the SETRAC simulations, whereas TOPKAPI only shows a minor reaction

Title Page

Abstract | Introduction

Conclusions | References

Tables | Figures

|◄ | ►|

◄ | ►

Back | Close

Full Screen / Esc

Printer-friendly Version

Interactive Discussion

on these sediment inputs. In the upper parts of the Chiene both models deliver almost identical results. TOPKAPI simulations with higher critical discharges (not shown here), e.g. by using Eq. (12) instead of 11, are closer to the observed bedload transport, but in several sections no transport is simulated due to a too high incipient motion criteria.

5　The observations cannot be reproduced. Considering an armour layer (Eq. 16) still overestimates the observations and compared to M1 there is only a small reduction of the total amount of bedload transported during the event (not shown here). It becomes obvious that losses due to form roughness are not negligible and are considered in model setups M2 and M3 with α equal to 1.5 (Fig. 6). Considering energy losses due

10　to form roughness delivers simulations closer to the observations. TOPKAPI produces higher bedload transport than SETRAC if M2 is taken. M3 uses the simulated discharge in Eq. (13) which is better suited for form losses estimates with rectangular cross-sections because the water level as used in Eq. (14) depends more on the bed structure than the discharge. Equation (13) is not implemented in SETRAC.

15　## 6　Comparison of SETRAC and TOPKAPI

For a detailed comparison of SETRAC and TOPKAPI we analysed the results of setup M1 without losses due to form roughness but with a variable bed (Fig. 7). SETRAC required around 9 h for the simulations, whereas TOPKAPI needed 40 s. In SETRAC the strip-wise solution of the flow routing and bedload transport requires several iterations.

20　The time step in SETRAC cannot be chosen by the user because the maximum allowed time step is calculated automatically to meet the Courant-Friedrichs-Lewy (CFL) stability criteria and is therefore not constant over the simulation time. During high discharges the time step becomes very small (1.5 s for the presented case study). The time step for sediment routing in TOPKAPI is also small (1 s) but it is only ap-

25　plied on the sediment routing scheme and not on the hydraulic simulations. These are performed on the grid level with an hourly time step. Figure 7 shows the transport capacities at 10, 30 and 60 h, the accumulated bedload transport, the channel

Title Page

Abstract　Introduction

Conclusions　References

Tables　Figures

◄　►

◄　►

Back　Close

Full Screen / Esc

Printer-friendly Version

Interactive Discussion

reach slopes and the depth of the sediment storage at the respective time step. The transport capacities produced by SETRAC show more fluctuations than the ones by TOPKAPI. TOPKAPI generally provides smaller transport capacities especially of the peaks at 3.5 and 7.0 km after 30 h. The variable slopes are comparable between the

5 two models, however especially at the last time step SETRAC exhibits pronounced fluctuations of the simulated slopes, whereas TOPKAPI delivers smoothed slopes along the channel. The sediment storage depths of TOPKAPI and SETRAC at 10 and 30 h correspond well. In the last time step, TOPKAPI's sediment depths are more fluctuating between 1 and 2.5 km compared to SETRAC and TOPKAPI simulates an empty

10 storage in the central part and upper reaches of the Chiene. SETRAC delivers fluctuating values between 0 and 1 m for these regions. A systematic difference between the two model outputs can be observed at the confluence of the Spigge and the Chiene at 6.0 km. Although, the bedload transport simulations downstream and upstream of the confluence point are almost identical between the two models, the cross-sections that

15 are directly affected by the confluence show significant differences. SETRAC delivers a much higher bedload transport and the sediment input from the tributary Spigge is clearly visible (peak at 6 km). TOPKAPI only shows a very moderate reaction to the additional sediment input.

7 Discussion

20 The reconstructed discharge is used to calibrate the two models. Since the overall goal of this study is to compare the newly developed sediment routing scheme of TOPKAPI with the well tested SETRAC model it is important to achieve a good fit between the two discharge simulations in order to make the sediment transport simulations comparable. This is achieved as shown in Fig. 5. For the comparison of modelled and reconstructed

25 bedload transport it is necessary to get the right water volumes. Therefore, the model results are compared to reconstructed discharge volumes based on gauging stations of the river Kander upstream and downstream of the confluence point of Chiene and

Title Page

Abstract | Introduction

Conclusions | References

Tables | Figures

◄ | ►

◄ | ►

Back | Close

Full Screen / Esc

Printer-friendly Version

Interactive Discussion

Kander. The reconstructed discharge must be viewed as an estimation which is prone to errors. The Chiene went out of its channel at the 22 August at 04:30 p.m. and therefore the maximum discharge of Chiene must have been higher than the reconstructed volumes. However, this additional volume cannot be estimated. Figure 5 shows that the reconstructed discharge volumes can be reproduced by both models.

Based on the LiDAR data we can only infer the net change after the event and no detailed temporal transport description is possible. Unfortunately, for extreme flood events in torrential channels such measurements are very difficult to obtain and detailed information on temporal changes of the streambed during an event are rarely available. The main purpose of this comparison to field data is to evaluate the performance of the simulation models along the channel and integrated over the flood event. The reconstructed bedload transport provides the order of magnitude of transported sediment volumes and it gives an idea of whether the macro roughness resistance has to be considered. We differenced the topography given by LiDAR data from before and after the event and summed to find net erosion and net deposition, and then equated this volume loss to a bedload transport flux. The accuracy of the LiDAR analyses is slope dependent (Scheidl et al., 2008) and therefore more accurate for milder reaches. The mean volume error can be determined by $0.3\,\text{m}^3/\text{m}^2$ for the analysed catchment (Chiari et al., 2009). There are several ways in which this method could be underestimating the actual bedload transport rates and reconstructed sediment budgets generally need to be handled with care. The event documentation (LLE Reichenbach, 2006) indicates that the reaches near and in the village of Kien on the alluvial fan were filled with sediment and the river left its bed during the raising limb of the flood hydrograph and deposited huge amounts of bedload in the village of Kien. The bedload transport calculated from morphologic changes can be regarded as lower boundary of the transported sediment volumes during the August 2005 flood, because it is not known how much sediment left the river outlet before the flow blockage. Fine sediments were deposited in depressions where lakes developed. Downstream of km 5.5 there was no major sediment input from tributaries. Therefore the field observations indicate that:

$$q_s(0) + \int (p_b(x))\, dx \ll \int \left(-(1 - \lambda_p)\frac{d\eta}{dt} \right) dx \qquad (19)$$

This means that our reconstruction approach covers the major sediment volumes redistributed during the event. Another source of uncertainty is that some sediment may have accumulated in between the LiDAR flights, primarily by hillslope processes, since no sediment transporting floods are documented for this period. Therefore, we consider the reconstructed bedload as estimation of the order of magnitude of the real transport rates.

As expected, both models significantly overestimate sediment transport if macro roughness resistance is not taken into account. The simulated bedload transport is up to 10 times higher than the reconstructed transport. Therefore, the accuracy of the reconstruction is good enough to evaluate the model setups M1, M2 and M3 and the comparison to the reconstructed bedload transport indicates that macro roughness resistance is probably non-negligible if modelling steep headwater streams. The transport capacity formulas were derived from laboratory flume experiments with more or less uniform bed materials. Therefore, they do not include effects of form drag due to irregular bed form structures. The energy losses due to form drag can be considered in the simulations and the parameter α is sensitive and requires a value of around 1.5 in order to provide an acceptable fit between the reconstructed and the simulated sediment transport. Discharge based macro roughness resistance corrections turned out to be better suited for the estimation of energy losses in the rectangular cross-sections of TOPKAPI. The finer river bed discretization of SETRAC enables a better simulation of the water levels whereas in TOPKAPI the water volume is equally distributed over the entire cross-section. The hydraulic simulations are done on the grid level with different channel geometry. This can cause significant differences in the water level although the discharge compares well between the two models.

The comparison of the two models revealed that differences can be observed at the confluence point of Spigge and Chiene. This is due to the spatial discretizations of the rivers on grid cell level and to differences in sediment transport simulations of the

Title Page

Abstract | Introduction

Conclusions | References

Tables | Figures

◀ | ▶

◀ | ▶

Back | Close

Full Screen / Esc

Printer-friendly Version

Interactive Discussion

Spigge. The confluence point of Spigge and Chiene and the lower cross-sections of Spigge are all covered by one grid cell which already holds the discharge contributions of the Spigge although on the sub-grid level the two rivers are still separated. There-fore, the Spigge sub-grid cross-sections were shifted upstream by one grid cell, which

5   means that no grid cell contains more than one river. This allows a better represen-tation of the hydraulic conditions. However, the real confluence point is located at the cross-section two grid cells further. Therefore, the flow conditions are different between the two spatial discretizations of SETRAC and TOPKAPI. Furthermore, the hydraulic simulations of the Spigge itself differ due to the predefined locations of the input hydro-

10 graphs of SETRAC. Figure 8a shows a significant jump of the accumulated water dis-charge at 0.8 km which is caused by a newly assigned hydrograph at this cross-section (SETRAC is limited by the number of hydrographs that can be assigned to a simulation system). TOPKAPI simulates more stable but lower potential transport rates, whereas SETRAC provides values almost three times higher than TOPKAPI (e.g. at 1.0 km in

15 Fig. 8b). This causes an increased deposition simulated by TOPKAPI between the confluence point and 0.5 km (Fig. 8d). The simulated sediment transport at the conflu-ence point of Spigge and Chiene is more than double in SETRAC (Fig. 8c). Therefore, less sediment is provided to the river Chiene in the TOPKAPI simulation, which is one reason for the lower sediment transport rates at the cross-sections downstream of the

20 confluence point. However, the different sediment fluxes of the Spigge cannot explain the entire difference between the two models. Simulation results of TOPKAPI with the sediment fluxes taken from SETRAC as input to the Chiene river at the confluence point provide an improvement (not shown here) and the peak becomes more visible but TOPKAPI still delivers bedload transport rates lower than SETRAC.

25 The fluctuations in SETRAC's bed slope calculations are more pronounced at lo-cations prone to bed erosion (Fig. 7). TOPKAPI simulates empty storages between 2.5 and 4.2 km and from 6.2 km upstream (Fig. 9a), whereas SETRAC still has fluctu-ating sediment storage depths between 0 and around 1 m, which can be explained by the wedge shaped erosion and deposition volumes calculated in SETRAC (see Chiari

2008 for details). The slope of TOPKAPI is equal to the bed rock slope in these areas as expressed in absolute differences between TOPKAPI, SETRAC and bed rock slopes in Fig. 9b. The most pronounced differences of SETRAC's slopes can be observed at the high erosion areas due to the fluctuating storage levels. The temporal develop-
ment of the slope in SETRAC shows similar slope patterns of the first and the last time step for reaches where the bed sediment is eroded. In depositional reaches the slope becomes more homogeneous, whereas in erosion reaches the channel gradient is shifted one cross-section downstream if the sediment storage is (nearly) emptied. The main difference between SETRAC and TOPKAPI is the wedge shaped sediment redistribution approach of SETRAC. TOPKAPI with its area-based erosion and deposi-tion simulations (sediment volumes are shifted from one cell to the other without further modifications as in SETRAC) delivers less fluctuations in erosion reaches but fluctua-tions can be observed in depositional reaches between 1 and 2.5 km in Fig. 9a.

The efficiency of the sub-grid modelling technique in TOPKAPI becomes obvious if simulation results of sediment transport on the grid level are compared to SETRAC (Fig. 10). For the simulations the sub-grid procedure was switched off and the simu-lations with mobile (solid line) and fixed (dashed line) river bed were conducted with setup M1. The geometrical information (width, initial slope and initial storage level) were taken from the cross-sections which are covered by the respective grid cells as mean values. The basic pattern of the SETRAC bedload transport simulations is re-produced (Fig. 10b), however lower transport rates are simulated. Interestingly, the model run with a fixed bed slope provides sediment transport rates closer to SETRAC than the one with variable bed slope especially between 0 and 5 km. However, the storage heights do not agree well with the SETRAC results (Fig. 10a). The analysis shows that the sub-grid modelling scheme significantly improves the simulation results. For first assessments sediment transport simulations on the grid level can already pro-vide estimates of acceptable reliability, especially if the significantly reduced amount of geometrical information is considered.

The effect of the sub-time step modelling is shown in Fig. 11. The relative number of redistributions in Fig. 11a is the total number of redistributions divided by the total number of time steps (number of sub-time steps × number of global time steps). The redistribution of additional sediment volumes in order to avoid blocking of the channel significantly reduces with increasing number of sub-time steps. With smaller time steps (e.g. 1 s), the transported sediment volume per time step is smaller than with larger time steps (e.g. 1 h), thus the chance to block the channel is smaller due to the mobile bed approach, which adjusts the slopes at the end of each time step. Interestingly, the redistributed sediment volumes in Fig. 11b already converge at a relatively small number of sub-time steps, n, and $n = 7$ (514.3 s) provides comparable total redistribution volumes as $n = 3600$ equivalent to 1 s. Thus the artificial redistribution can be minimized by a sufficiently small sub-time step.

8 Conclusions and outlook

The newly implemented sediment transport module in the distributed hydrological model TOPKAPI enables the simulation of sediment transport rates, erosion and deposition patterns and bed slope developments in a river channel network. Since the transport module is directly coupled to the hydrological model, effects of changes in the hydrological cycle on the sediment transport patterns can be studied. The performance of TOPKAPI compared to a more sophisticated, specialized sediment transport model (SETRAC) is satisfying. The advantages and disadvantages of the two models are listed in Table 2. The major innovation of this study is the implementation of the sub-grid modelling scheme, which significantly improves the simulation of the sediment transport. The stationary assumption that discharge can be simulated on the grid level and taken for all sub-grid sections within that grid cell provides reliable discharge values for the sediment transport simulations. This approach exhibit inaccuracies at confluence points, for which a more sophisticated solution for flow portioning should be used based on the ratio of inflowing discharge from the upstream cells. TOPKAPI does

not consider a feedback mechanism of the mobile bed on the hydraulic simulations. This limitation can be taken into account if the slope changes are moderate during an event. However, an up-scaling of the sub-grid geometry should be investigated further. In a first step average values of the geometrical features (slopes) could be used to couple the hydraulics on the grid level with the sediment transport simulations on the sub-grid level. The computations in TOPKAPI are quite efficient and the model requires only 40 se on a standard desktop computer for the simulation of the 60 h event with 3600 sub-time steps. An artificial redistribution of sediment by transferring additional sediment volumes to the next downstream cell is necessary to avoid blocking of the channel and to ensure positive downstream bed slopes. However, the routing of the additional sediment volume to the downstream cell cannot be explained physically because the transport capacity is already exceeded in the time step in which the redistribution takes place. The mechanism can be partly avoided by a small sub-time step.

References

Bahadori, F., Ardeshir, A., and Tahershamsi, A.: Prediction of alluvial river bed variation by SDAR model, J. Hydraul. Res., 44(5), 614–623, 2006.

Badoux, A. and Rickenmann, D.: Berechnung zum Geschiebetransport während der Hochwasser 1993 und 2000 im Wallis, 100. Jahrgang, Wasser Energie Luft, 3, 217–226, 2008.

Beffa, C.: 2D-Simulation der Sohlenreaktion in einer Flussverzweigung, Österreichische Wasser- und Abfallwirtschaft, 42(1–2), 1–6, 2005.

Brock, B., Willis, I., and Sharp, M.: Measurement and parametrization of albedo variations at Haut Glacier d'Arolla, Switzerland, J. Glaciol., 46(155), 675–688, 2000.

Chiari, M.: Numerical modelling of bedload transport in torrents and mountain streams, PhD dissertation, University of Natural Resources and Applied Life Sciences, Vienna, Austria, 2008.

Chiari, M., Scheidl, C., and Rickenmann, D.: Assessing morphologic changes caused by torrential flood events with airborne lidar data, in: Land conservation – LANDCON 0905, Proceedings on CD, 8 pp., 2009.

Chiari, M., Friedl, K., and Rickenmann, D.: A one dimensional bedload transport model for steep slopes, J. Hydraul. Res., 48(2) 152–160, doi:10.1080/00221681003704087, 2010.

Chow, V. T., Maidment, D. R., and Mays, L. W.: Applied hydrology, Civil Engineering Series, McGraw-Hill Book Company, 1988.

Corripio, J. G.: Vectorial algebra algorithms for calculating terrain parameters from DEMs and solar radiation modelling in mountainous terrain, Int. J. Geogr. Inf. Sci., 17(1), 1–23, 2003.

Deyhle, C., Glugla, G., Golf, W., v. Hoyningen Huene, J., Kalweit, H., Olbrisch, H., Richter, D., Wendling, U., Wessolek, G., and Wittenberg, H.: Ermittlung der Verdunstung von Land- und Wasserflächen, Technical Report 238, Deutscher Verband für Wasserwirtschaft und Kulturbau e.V. (DVWK), 1996.

Doten, C. O., Bowling, L. C., Lanini, J. S., Maurer, E. P., and Lettenmaier, D. P.: A spatially distributed model for the dynamic prediction of sediment erosion and transport in mountainous forested watersheds, Water Resour. Res., 42, W04417, doi:10.1029/2004WR003829, 2006.

Fehr, R.: A method for sampling very coarse sediments in order to reduce scale effects in movable bed models, Proc. Symp. Scale effects in modelling sediment transport phenomena, Toronto, IAHR, Delft, 383–397, 1986.

Hassan, M. A., Church, M., and Lisle, T. E.: Sediment transport and channel morphology of small, forested streams, J. Am. Water Resour. Assoc., 41(4), 853–876, 2005.

Hock, R. and Noetzli, C.: Areal melt and discharge modelling of Storglaciaren, Sweden, Ann. Glaciol., 24, 211–216, 1997.

Liu, Z. and Todini, E.: Towards a comprehensive physically-based rainfall-runoff model, Hydrol. Earth Syst. Sci., 6, 859–881, doi:10.5194/hess-6-859-2002, 2002.

Liu, Z., Martina, M. L. V., and Todini, E.: Flood forecasting using a fully distributed model: application of the TOPKAPI model to the Upper Xixian Catchment, Hydrol. Earth Syst. Sci., 9, 347–364, doi:10.5194/hess-9-347-2005, 2005.

Lokale lösungsorientierte Ereignisanalyse (LLE) Reichenbach: Technischer Bericht, Emch + Berger AG, Spiez; Hunziker, Zarn & Partner AG, Aarau; Geotest AG, Zollikofen; Tiefbauamt Kanton Bern, Bern, 2006.

Mathys, N., Brochot, S., Meunier, M., and Richard, D.: Erosion quantification in the small marly experimental catchments of Draix (Alpes de Haute Provence, France): Calibration of the ETC rainfall-runoff-erosion model, Catena, 50, 527–548, 2003.

MeteoSchweiz: Starkniederschlagsereignis August 2005, Arbeitsberichte der MeteoSchweiz 211, Bundesamt für Meteorologie und Klimatologie, 63 pp., 2006.

Meyer-Peter, E. and Mueller, R.: Formulas for bedload transport, 2nd IAHR Congress, Stockholm, Appendix 2, 39–64, 1948.

Papanicolaou, A., Bdour, A., and Wicklein, E.: One-dimensional hydrodynamic/sediment transport model applicable to steep mountain streams, J. Hydraul. Res., 42(4), 357–375, 2004.

Pellicciotti, F., Brock, B., Strasser, U., Burlando, P., Funk, M., and Corripio, J.: An enhanced temperature-index glacier melt model including the shortwave radiation balance: development and testing for Haut Glacier d'Arolla, Switzerland, J. Glaciol., 51(175), 573–587, 2005.

Reichel, G., Fäh, R., and Baumhackl, G.: FLORIS-2000: Ansätze zur 1.5 Dsimulation des Sedimenttransportes im Rahmen der mathematischen Modellierung von Fließvorgängen, in: Internat. Symposion "Betrieb und Überwachung wasserbaulicher Anlagen", 2000.

Rickenmann, D.: Bedload transport capacity of slurry flows at steep slopes, Mitteilung 103, Versuchsanstalt für Wasserbau, Hydrologie Glaziologie, ETH Zurich, Zurich, 1990.

Rickenmann, D.: Hyper-concentrated flow and sediment transport at steep slopes, J. Hydraul. Eng., 117(11), 1419–1439, 1991.

Rickenmann, D.: An alternative equation for the mean velocity in gravel-bed rivers and mountain torrents, in: Proc. Nat. Conf. Hydraulic Engineering, edited by: Cotroneo, G. V. and Rumer, R. R., Buffalo NY 1, ASCE, New York, 672–676, 1994.

Rickenmann, D.: Fliessgeschwindigkeit in Wildbächen und Gebirgsflüssen, Wasser Energie Luft, 88(11/12), 298–304, 1996.

Rickenmann, D.: Comparison of bed load transport in torrents and gravel bed streams, Water Resour. Res., 37(12), 3295–3305, 2001.

Rickenmann, D., Chiari, M., and Friedl, K.: SETRAC – A sediment routing model for steep torrent channels, River Flow 2006 1, edited by: Ferreira, R., Leal, E. A. J., and Cardoso, A., Taylor & Francis, London, 843–852, 2006.

Distributed physically based hydrological catchment model

M. Konz et al.

Title Page

Abstract	Introduction
Conclusions	References
Tables	Figures

|◄ | ►|

◄ | ►

Back | Close

Full Screen / Esc

Printer-friendly Version

Interactive Discussion

Rinderer, M., Jenewein, S., Senfter, S., Rickenmann, D., Schöberl, F., Stötter, J., and Hegg, C.:. Runoff and bedload transport modelling for flood hazard assessment in small alpine catchments – the PROMAB-GIS model, in: Sustainable Natural Hazard Management in Alpine Environments, edited by: Veulliet, E., Stötter, J., and Weck-Hannemann, H., Springer, Heidelberg, New York, 69–101, 2009.

Scheidl, C., Rickenmann, D., and Chiari, M.: The use of airborne LiDAR data for the analysis of debris flow events in Switzerland, Nat. Hazards Earth Syst. Sci., 8, 1113–1127, doi:10.5194/nhess-8-1113-2008, 2008.

Todini, E. and Ciarapica, L.: The TOPKAPI model, in: Mathematical models of large watershed hydrology, edited by: Singh, V. P., Water Resources Publications, Littleton, Colorado, USA, 2001.

Todini, E. and Mazzetti, C.: TOPKAPI User manual and references, PROGEA, 2008.

Wicks, J. M. and Bathurst, J. C.: SHESED:Aphysically based, distributed erosion and sediment yield component for the SHE hydrological modelling system, J. Hydrol., 175, 213–238, 1996.

Distributed physically based hydrological catchment model

M. Konz et al.

Title Page

Abstract	Introduction
Conclusions	References
Tables	Figures

|◄ | ►|

◄ | ►

Back | Close

Full Screen / Esc

Printer-friendly Version

Interactive Discussion

Distributed physically based hydrological catchment model

M. Konz et al.

Table 1. Model setups of TOPKAPI and SETRAC used to simulate the 2005 event. M3 was only used for TOPKAPI.

Model setup	Bedload transport	Incipient motion	Form roughness	Exponent α
M1	Eq. (10)	Eq. (11)	–	–
M2	Eq. (10)	Eq. (11)	Eq. (14)	1.5
M3	Eq. (10)	Eq. (11)	Eq. (13)	1.5

Table 2. Advantages and disadvantages of TOPKAPI and SETRAC.

	TOPKAPI	SETRAC
Advantages	CPU time	Detailed representation of channel cross-sections
	Direct coupling of hydrological and channel processes	Graphical user interface with many visualization possibilities and geo-referenced representation of the channel network
	Simulations in different spatial scales	Internal discretization selectable by the user for sensitivity analysis
		No selection of calculation time step required (model decides on the maximum allowed time step for stable calculation)
		One grain model and fractional bedload transport calculations
		Results can be stored as preformatted A0 DXF files for practical applications and as text files for detailed analysis
Disadvantages	Only rectangular channel geometry	CPU time
	Artificial redistribution in order to avoid blocked channels	External simulations of the hydrology required

Limited to steep mountain rivers due to kinematic wave approximation
No counter slopes or backwater effects considered
Limited to bedload transport (no suspended load or washload)

Discussion Paper | Discussion Paper | Discussion Paper | Discussion Paper | Discussion Paper

HESSD

7, 7591–7631, 2010

Distributed physically based hydrological catchment model

M. Konz et al.

Title Page

Abstract | Introduction

Conclusions | References

Tables | Figures

|◄ | ►|

◄ | ►

Back | Close
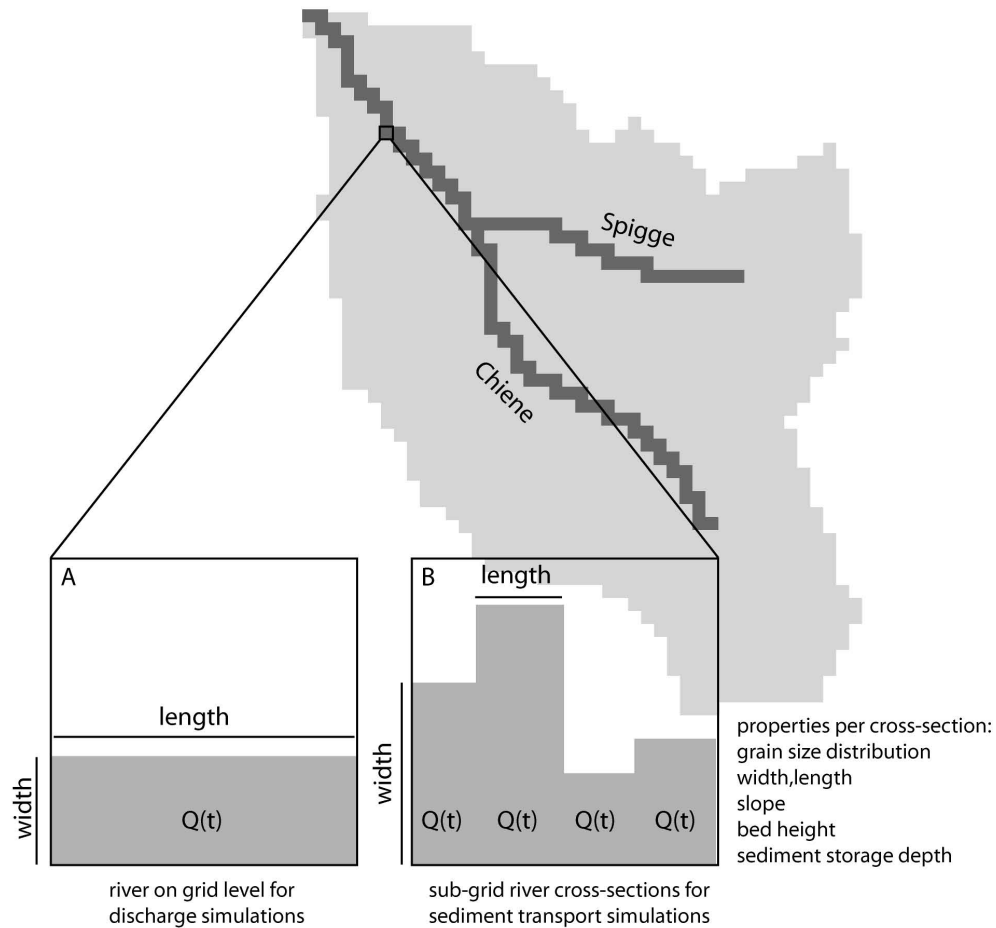
Full Screen / Esc

Printer-friendly Version

Interactive Discussion

Fig. 1. Chiene catchment area and location of gauging stations for discharge reconstruction.

Fig. 2. Properties of the Chiene river and observations of bedload transport. **(A)** Reconstructed bedload transport, **(B)** initial depth of sediment storage, **(C)** bed slope of the river and channel width.

Fig. 3. Sub-grid concept of river cross-sections. **(A)** River representation for hydraulic simulations on the grid level; **(B)** sub-grid cross-sections for sediment transport simulations.

Title Page

Abstract | Introduction

Conclusions | References

Tables | Figures

|◀ | ▶|

◀ | ▶

Back | Close

Full Screen / Esc

Printer-friendly Version

Interactive Discussion
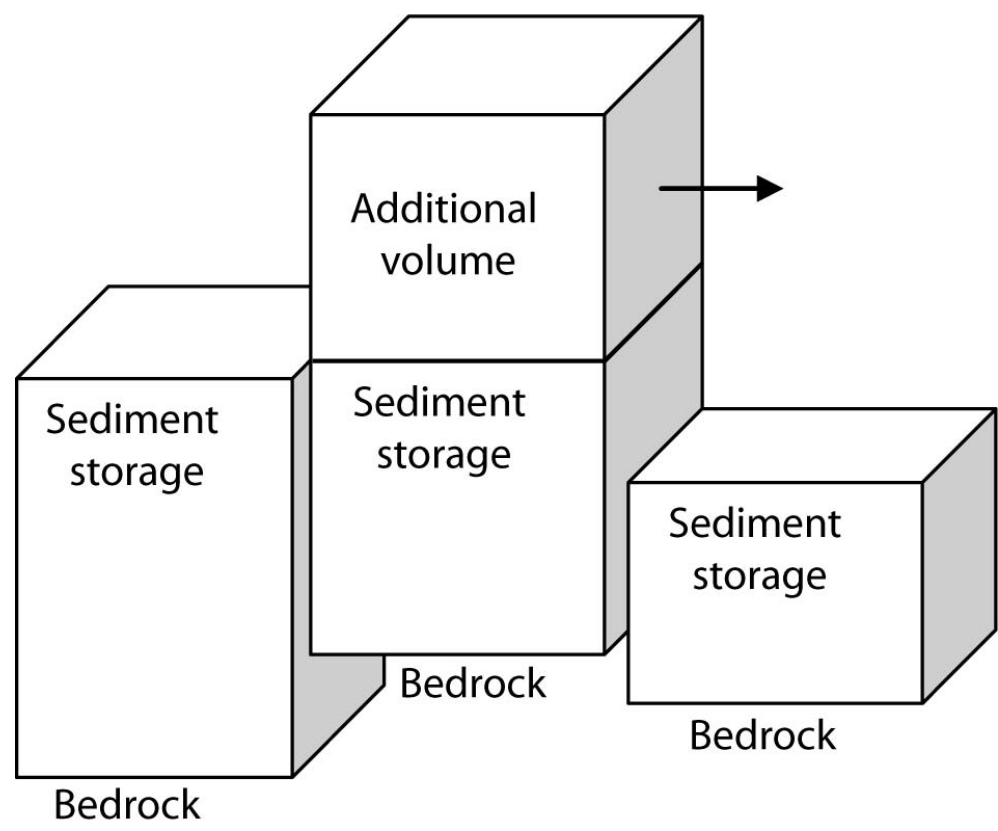
Fig. 4. Redistribution of additional sediment volumes in order to avoid upward slopes.
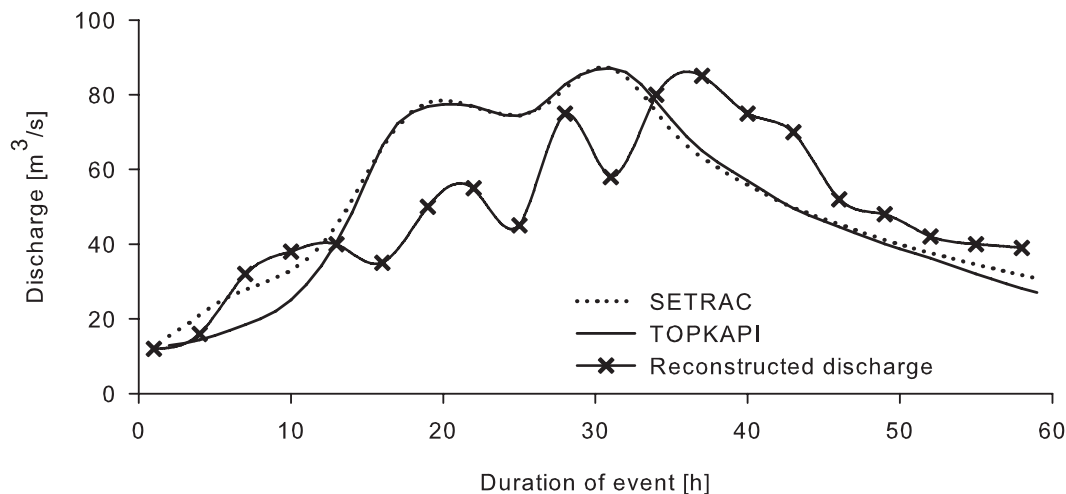
Fig. 5. Comparison of reconstructed discharge with TOPKAPI and SETRAC simulations of the event at 21 to 23 August 2005 for sediment transport calculations with initial conditions taken from long-term simulations.

Title Page

Abstract | Introduction

Conclusions | References

Tables | Figures

◄ | ►

◄ | ►

Back | Close

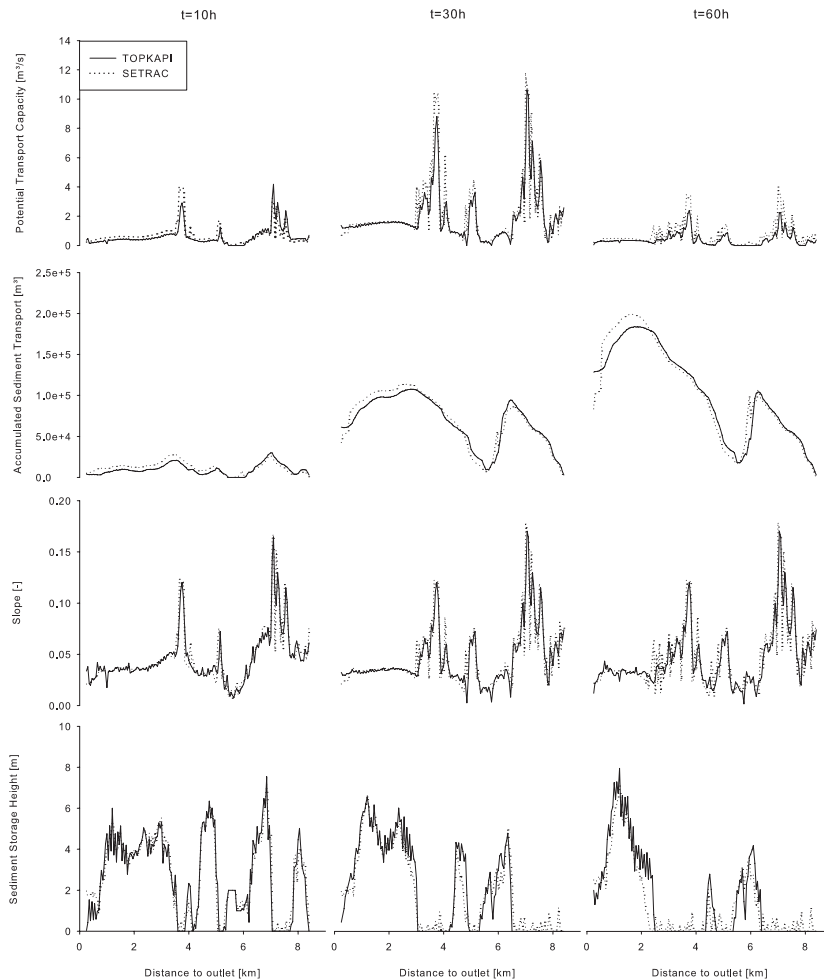Full Screen / Esc

Printer-friendly Version

Interactive Discussion
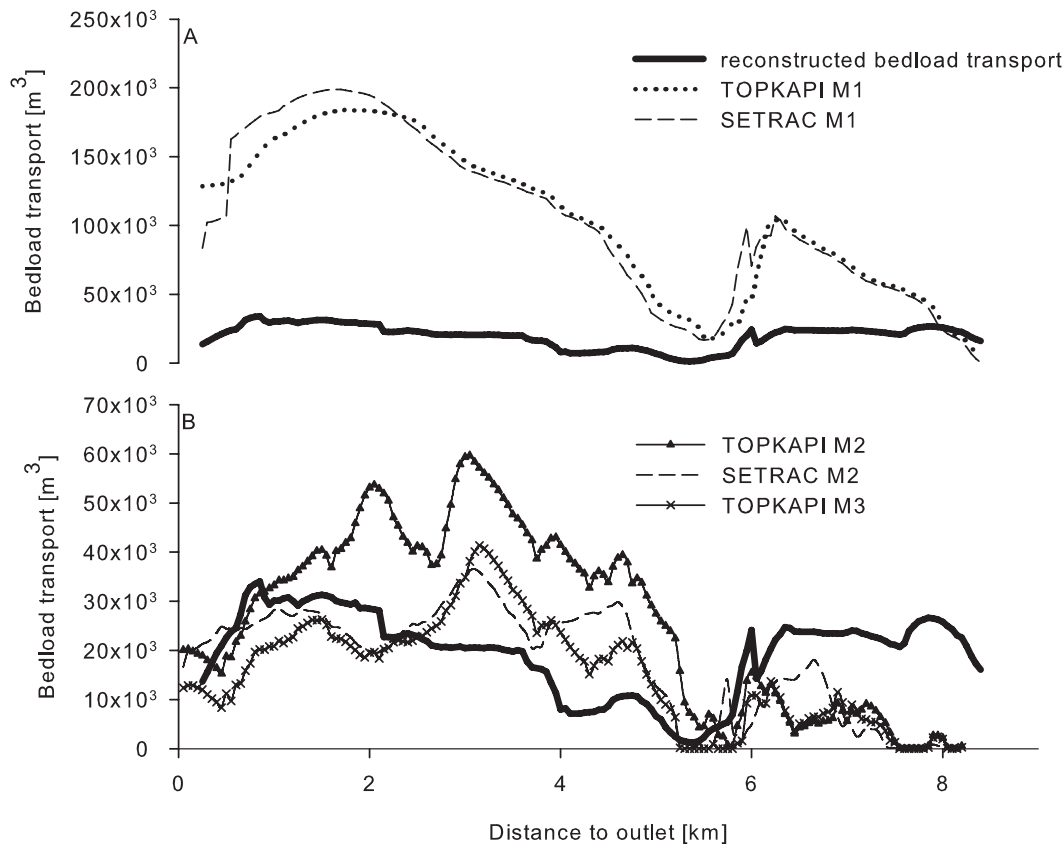
Fig. 6. Comparison of TOPKAPI, SETRAC and reconstructed bedload transport. Simulations were done with different setups described in Table 1. **(A)** Simulations with full transport capacity (M1), **(B)** simulations considering losses due to form roughness using setups M2 and M3. Equation (13) is not implemented in SETRAC and therefore M3 is only used for TOPKAPI simulations.

Title Page

Abstract | Introduction

Conclusions | References

Tables | Figures

|◄ | ►|

◄ | ►

Back | Close

Full Screen / Esc

Printer-friendly Version

Interactive Discussion

Fig. 7. Detailed comparison of TOPKAPI and SETRAC for setup M1.
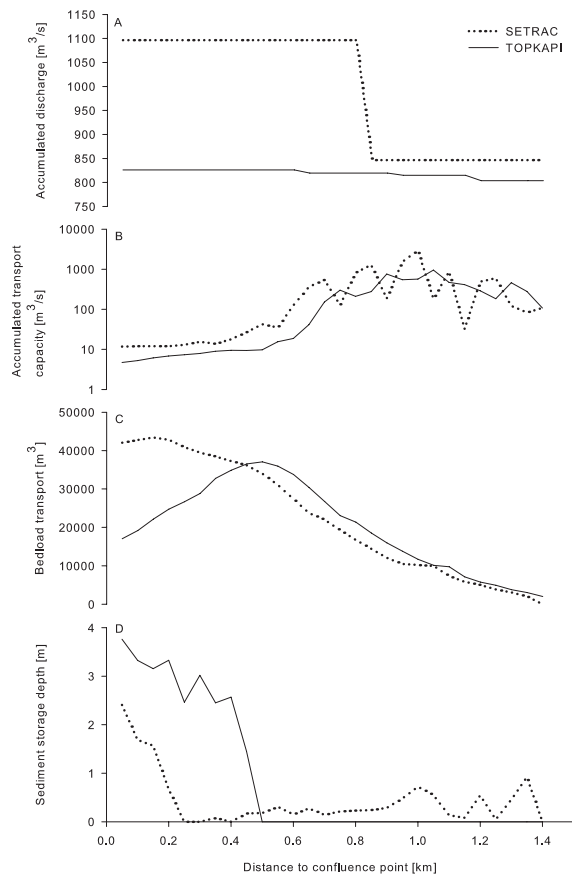
Fig. 8. Comparison of SETRAC and TOPKAPI for the tributary Spigge. **(A)** Accumulated discharge over the simulation period for each cross-section element, **(B)** accumulated transport capacity, **(C)** bedload transport of each cross-section of the entire simulation period, **(D)** sediment storage depth of the last time step.
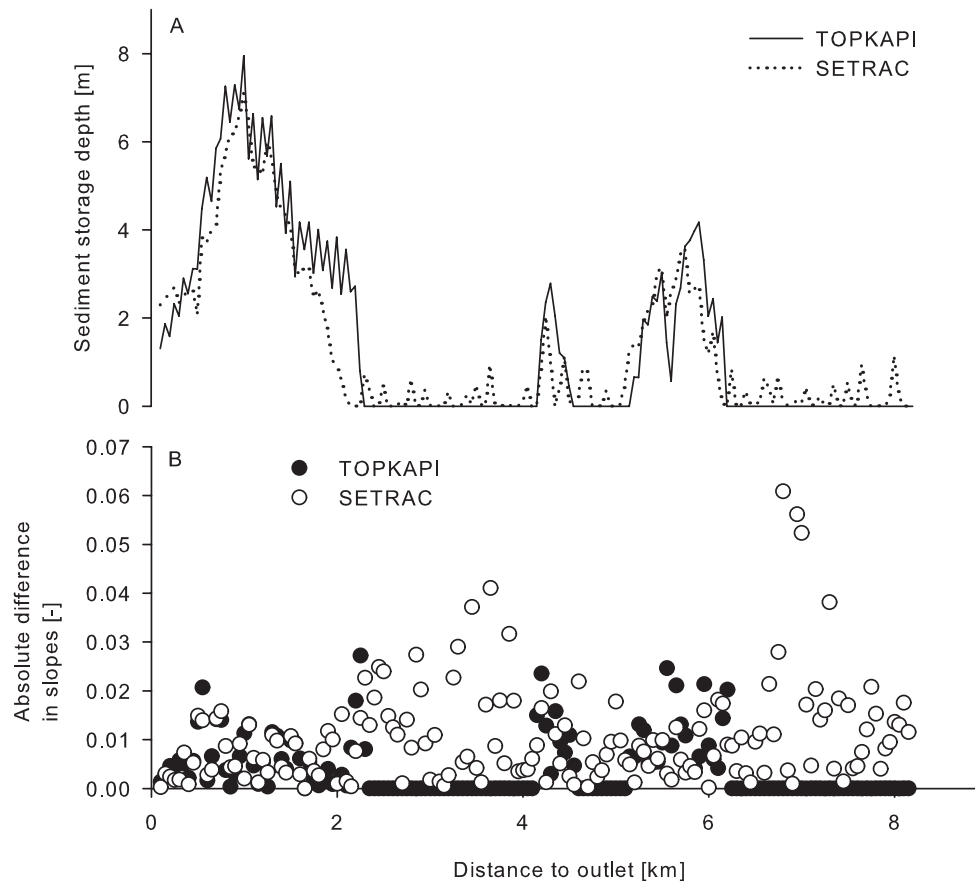
Fig. 9. Comparison of sediment storage depths and slope developments of SETRAC and TOP-KAPI. **(A)** Simulated sediment storage depths by TOPKAPI and SETRAC for the last simulation time step; **(B)** absolute differences between the bed rock slope and the slopes provided by TOPKAPI and SETRAC for the last simulation time step.
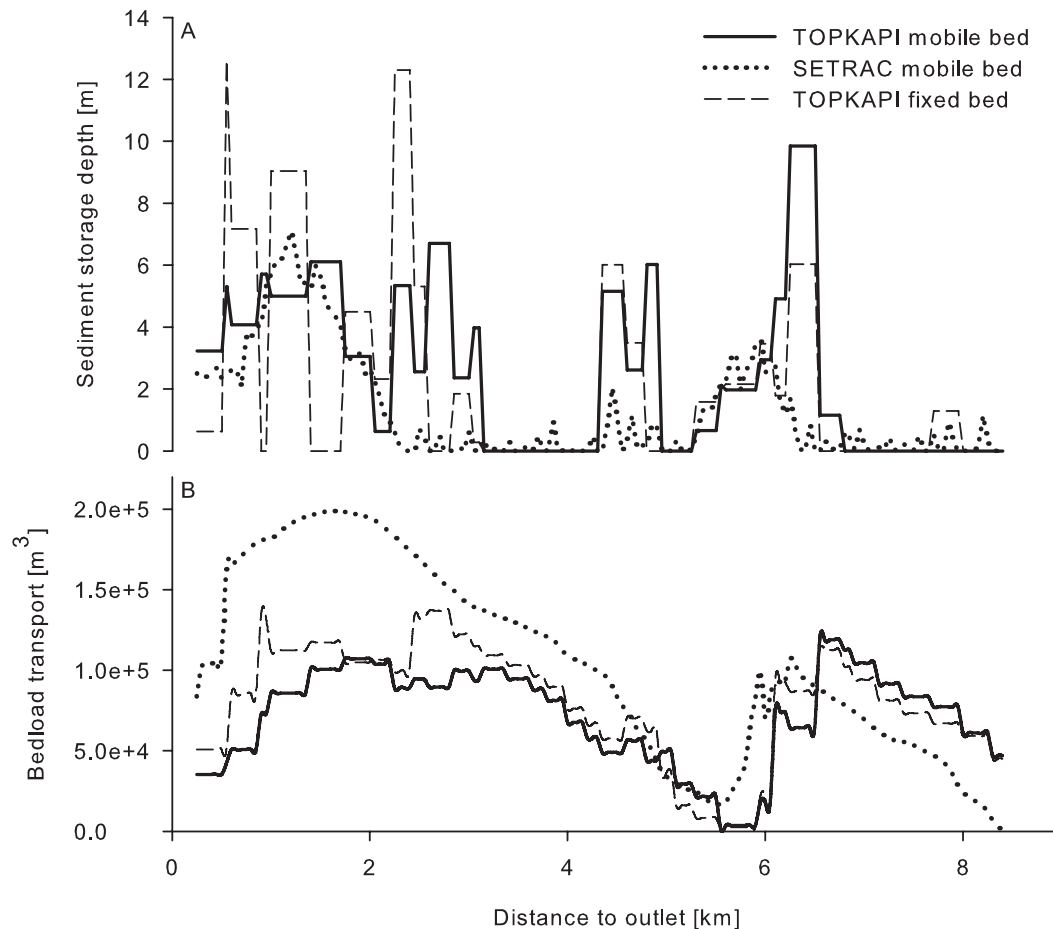
Fig. 10. Comparison of sediment transport simulations of TOPKAPI on the grid level with SETRAC. **(A)** Simulated sediment storage depths (with mobile and fixed beds); **(B)** bedload transport without form losses.

Discussion Paper | Discussion Paper | Discussion Paper | Discussion Paper

HESSD

7, 7591–7631, 2010

Distributed physically based hydrological catchment model

M. Konz et al.

Title Page

Abstract | Introduction

Conclusions | References

Tables | Figures

◀ | ▶

◀ | ▶

Back | Close

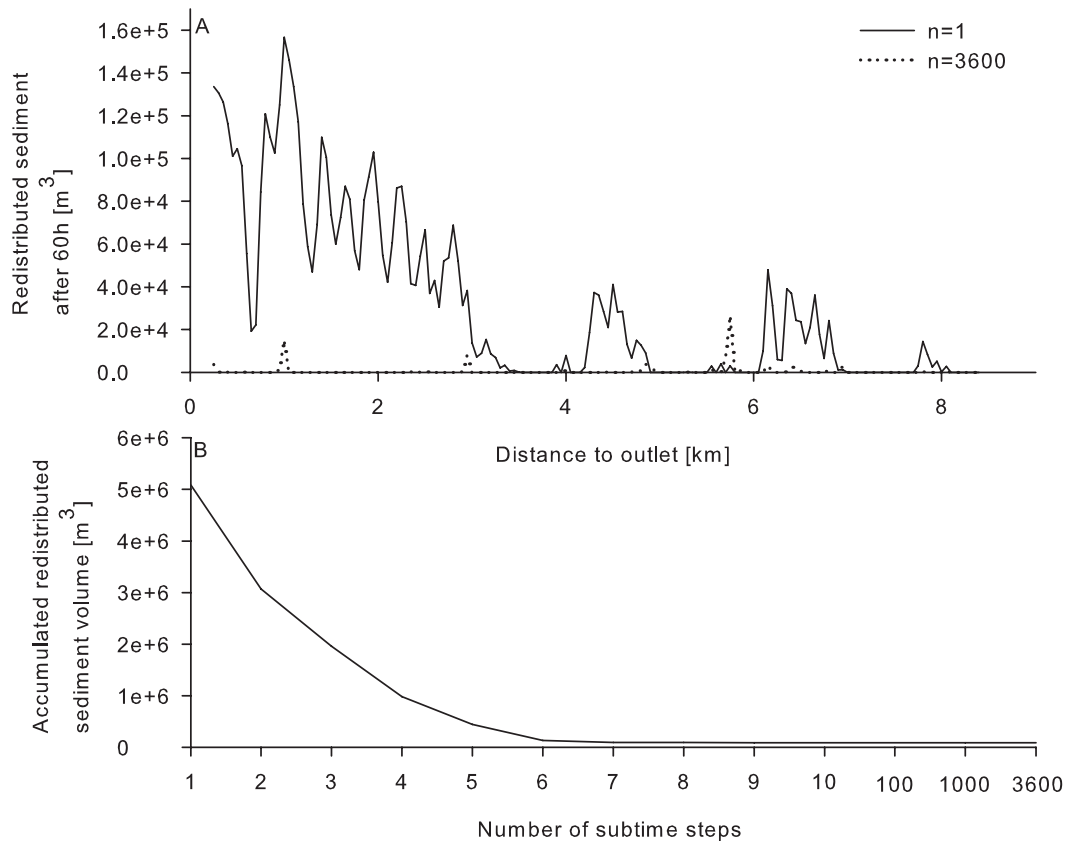Full Screen / Esc

Printer-friendly Version

Interactive Discussion

Fig. 11. Effect of sub-time step modelling. **(A)** Relative number of artificial sediment redistributions along the channel; **(B)** accumulated, redistributed sediment volumes simulated with different temporal resolutions.

Title Page

Abstract | Introduction

Conclusions | References

Tables | Figures

|◄ | ►|

◄ | ►

Back | Close

Full Screen / Esc

Printer-friendly Version

Interactive Discussion